October 1996 • NREL/TP-451-21704

Photocharge Transport and Recombination Measurements in Amorphous Silicon Films and Solar Cells by Photoconductive Frequency Mixing

Annual Subcontract Report 15 May 1995 - 15 May 1996

R. Braunstein and S. Dong
University of California
Los Angeles, California

National Renewable Energy Laboratory
1617 Cole Boulevard
Golden, Colorado 80401-3393
A national laboratory of the U.S. Department of Energy
Managed by Midwest Research Institute
for the U.S. Department of Energy
under Contract No. DE-AC36-83CH10093

NREL/TP-451-21704 • UC Category: 1260 • DE96013112

Photocharge Transport and Recombination Measurements in Amorphous Silicon Films and Solar Cells by Photoconductive Frequency Mixing

Annual Subcontract Report 15 May 1995 - 15 May 1996

R. Braunstein and S. Dong
University of California
Los Angeles, California

NREL technical monitor: B. von Roedern

National Renewable Energy Laboratory
1617 Cole Boulevard
Golden, Colorado 80401-3393
A national laboratory of
the U.S. Department of Energy
Managed by Midwest Research Institute
for the U.S. Department of Energy
under Contract No. DE-AC36-83CH10093

Prepared under Subcontract No. XAN-4-13318-10
October 1996

Available to DOE and DOE contractors from:
Office of Scientific and Technical Information (OSTI)
P.O. Box 62
Oak Ridge, TN 37831
Prices available by calling (423) 576-8401

Available to the public from:
National Technical Information Service (NTIS)
U.S. Department of Commerce
5285 Port Royal Road
Springfield, VA 22161
(703) 487-4650

Preface

The prime candidate material for thin-film photovoltaic high efficient solar cells for large-scale power generation is hydrogenated amorphous silicon and alloys. The objectives of the technology in this field are to achieve stable and efficient units for cost effective bulk-power generation. The strategy in this field is to optimize amorphous thin-film growth for greater efficiency and the reduction of light-induced instability. Material preparation efforts of amorphous semiconductors have concentrated on the reduction of "Urbach" edges, sub-bandgap absorption, and the density of deep defects to the end to maximize the photoconductive gain of the material. Most material efforts have been to optimize mobility-lifetime product ($\mu\tau$) as measured by steady state photoconductivity which does not determine μ and τ separately. To evaluate various photocharge transport models, it is essential that a simultaneous determination of the mobility and lifetime be performed so as to predict the performance of solar cells. We have developed a photomixing technique to separately determine the mobility and lifetime to characterize materials to predict solar cell performance and to allow the testing of new materials and devices in actual solar cell configurations. The present program forms part of the NREL High-Bandgap Alloy Team and the Metastability and the Mid-bandgap Alloy Team. Various groups are concerned with material synthesis and device fabrication. The UCLA Group performs photoconductive frequency mixing measurements on these material and solar cell devices to determine the optimum growth conditions for photocharge transport. The continuous feedback of the results of the UCLA Group aids synthesis and relates material properties to device performance and gain insight into the light-induced degradation mechanisms.

Table of Contents

List of Figures

List of Tables

Summary

The transport properties of intrinsic hydrogenated amorphous silicon samples with the hydrogen content ranging from over 10% to less 1%, which were produced by the hot-wire technique at NREL, were systematically studied by the photomixing technique.

The continuous decay of electron drift mobility in intrinsic hydrogenated amorphous silicon (a-Si:H) upon light soaking was investigated. The degradation of photoconductivity, lifetime and drift mobility in these a-Si:H samples while light-soaking were determined. In addition to the decay of the photoconductivity and electron lifetime, continuous decay of the electron drift mobility was found during the light soaking process, which reveals a new phenomenon associated with the Staebler-Wronski effect. The drift mobility decreased by a factor of 2 - 4 for 5 hour light soaking at 4 sun intensity. Experimental data were fitted to a stretched exponential law. Different stretched-exponential parameters for photoconductivity, lifetime and drift mobility were obtained, which indicates the production of defects with different generation kinetics upon light soaking.

The effects of deposition conditions on transport properties of intrinsic a-Si:H films were investigated. By using the photomixing technique, we have determined the electron drift mobility, lifetime and the conduction band Urbach energy (~ 0.1 eV below the band edge) of a-Si:H films as a function of substrate temperature ($290C \le T_s \le 400C$). We have found that with increasing substrate temperature, the lifetime, the drift mobility and the photoconductivity decreased but the Urbach energy increased; these results, together with previous results of other workers, indicate that for the a-Si:H films with increasing deposition temperature, the density of positively charged, negatively charged, and neutral defects all show a tendency to increase.

We have found that the drift mobility (μ_d) of these samples increases, the lifetime (τ) decreases with increasing electric field, while the $\mu\tau$ product is essentially independent of the electric field in the range of 1000V/cm - 10,000V/cm. For all of these samples, the electric field dependence of mobility $(\Delta\mu)/\mu_0/(\Delta E)$ in the as-grown or/and annealed states are always larger than that in the light soaked state. The electric field dependence of mobility can be explained by the existence of long-range potential fluctuations. Employing a model for potential fluctuations, which we have previously reported, we obtained the ranges of the fluctuations in these samples for the as-grown, annealed and light soaked states. For all of these samples, the ranges of potential fluctuations in as-grown or/and annealed states are always longer than in the light soaked state. In addition, we have found that the electric field dependence of mobility could be different between as-grown and annealed states. It indicates that the concentration or nature of the defects in the as-grown and in the annealed states could be different which depends on the process of produce.

Preliminary measurements, which have been performed on two Schottky structure samples fabricated with PEVCD (TPni48) and hot-wire (THDni50) intrinsic layers respectively, show that the photomixing technique can be extended to solar cell devices. It is possible to deduce the following parameters: the products of the thickness of depletion layer and absorption coefficient, the barrier potential and the transit time.

Introduction

The research pursued during Phase II was part of a collaboration with members of the NREL the Metastability and Mid-bandgap Alloy Team. The tasks were concerned with the characterization of the photoconductivity as a function of temperature and electric field of a series of a-Si:H layers so as to deconvolute the mobility-lifetime products into mobility and lifetime. In addition, the details of the changes of the above parameters as a function of light induced degradation were investigated. Evidence for the continuous decay of the electron drift mobility in intrinsic a-Si:H upon light soaking was obtained by the photomixing technique. In addition the effect of deposition temperature on the transport properties of intrinsic a-Si:H was also investigated. The dominant approach to accomplish the tasks of the present phase of the program is the technique of photoconductive frequency mixing to separately determine the drift mobility and lifetime. In the following sections, the theory of the photoconductive frequency mixing (photomixing), the experimental configuration and the results of the light degradation studies and the characterization of the photocurrent properties of a-Si:H are presented. The transport properties of intrinsic hydrogenated amorphous silicon samples with hydrogen contents ranging from over 10% to less 1%, which were produced by hot-wire technique at NREL, were systematically studied by the photomixing technique. Other measurements on similar samples are being performed by Dr. Crandall's group using CPM and by Dr. Cohen's group using capacitance measurements. These enable a correlation of the properties determined by different techniques.

This report describes work performed during the phase II of the program in a number of areas. The technique of photoconductive frequency mixing was employed to separately determine the mobility and lifetime in a-Si:H. Light induced degradation studies reveal that in addition to the decay of the photoconductivity and electron lifetime, a continuous decay of the electron drift mobility is observed during the light soaking process, which reveals a new phenomenon associated with the Staebler-Wronski effect. In addition to the generation of defects as recombination centers, charged defects acting as scattering centers can also be generated upon light soaking. Different generation kinetics for these two kinds of defects were found through stretched-exponential-law analyses. The charged scattering centers can be formed from deep trapping or recombination centers through some relaxation processes.

The effects of deposition temperature in the transport properties of a-Si:H were investigated. Our results, together with previous results of other workers, indicate that for the a-Si:H films with increasing deposition temperature, the density of the defects increases. The photomixing technique, which can experimentally determine both the drift mobility and lifetime, together with subgap absorption, can provide information not only for the density of midgap defects, but also for the charge state profile of midgap defects.

Measurements of the electric field dependence of the drift mobility indicate that the electric field dependence of mobility $(\Delta\mu)/\mu_0/(\Delta E)$ in as-grown or/and annealed states are always larger than that in light soaked state and the concentration or nature of the defects in the as-grown and in the annealed states could be different which depend on the process of produce.

Brief Description of Photomixing Technique for Separate Determination of Mobility and Lifetime

We have developed a photomixing technique that allows us to determine both drift mobility and lifetime. This technique has been successfully applied to single crystalline, polycrystalline and amorphous semiconductors, such as c-Si[1], a-Si:H[2-5], a-SiC:H[4], a-As_2Te_3[6] and polycrystalline $CuInSe_2$[7].

The photomixing technique employed is based on the idea of heterodyne detection for photoconductors. When two similarly polarized monochromatic optical beams of slightly different frequencies are incident upon a photoconductor, the generation rate of electron-hole pairs and therefore the photocurrent produced, when a dc bias is applied, will contain components resulting from the square of the sum of the incident electrical fields. Consequently, a photocurrent composed of a dc and a microwave current due to the beat frequency of the incident fields will be produced; these two photocurrents allow a determination of the mobility and lifetime of the photo-generated carriers according following equations:

$$\mu_d = \omega \sqrt{\langle \sigma_{ac}^2 \rangle} / \left(\sqrt{2} e G_0 \lambda \right) \tag{1}$$

$$\tau = \sigma_{dc} / (e G_0 \mu_d) \tag{2}$$

In the present work, instead of using two lasers, the multiple longitudinal modes of a single laser were used. In the above ω is the photomixing angular frequency (~ 1.58 GHz, corresponding to a time scale of ~ 630 ps), λ (~ 7.05%) is an effective modulation index, G_0 is the dc electron-hole pair generation rate, σ_{dc} is the dc photoconductivity, and $\sqrt{\langle \sigma_{ac}^2 \rangle}$ is the root-mean-square ac photoconductivity which is determined by the power of the microwave photomixing signal.

Experimental setup of photomixing

The block diagram of the experimental setup for photomixing is shown in Fig. 1. The dc photo-signal was measured by a Keithley 617 Programmable Digital Electrometer, and the photomixing signal, i.e., the ac photo-signal, was measured by a Tektronix 492P Spectrum Analyzer. The dc and the ac signals were separated by a low pass filter and a high pass filter, which are incorporated in a bias tee, that was connected to a three stub tuner. By tuning the stub tuner, the reflection of the photomixing signal, which is in the microwave range, from the Spectrum Analyzer can be reduced to nearly zero, and thus the true measurements of the photomixing signal can be achieved. All the equipment were controlled by an IBM PC through a National Instruments Lab-

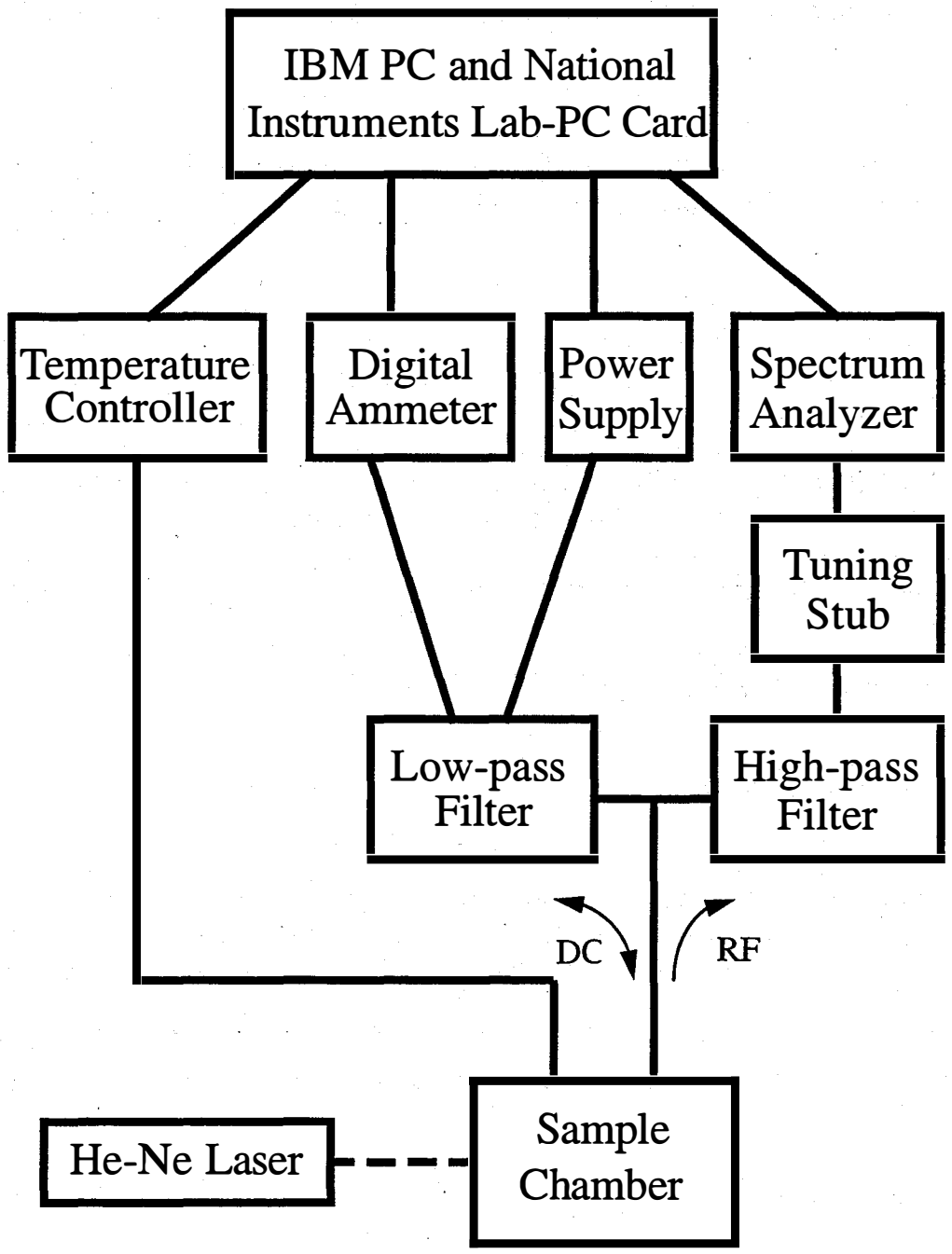

Figure 1. Block diagram of the experimental setup for photomixing.

PC card.

A Spectra-Physics 125A He-Ne laser was used as the light source. the laser beam can also be focused onto the sample for photomixing measurements *in situ* with light soaking.

Result and analysis

Light induced degradation and continuous decay of drift mobility in intrinsic a-Si:H upon light soaking

The intrinsic a-Si:H samples, provided by the National Renewable Energy Laboratory (NREL), were deposited by hot-wire technique[8] on Corning 7059 glass. The basic properties of samples of two batches produced at different times are listed as follow:

Table 1. Sample characterization of samples THD58-61 and THD82-83

Sample ID	Substrate Temp.(C)	Heater Temp.(C)	H Content (%)	Thickness (μm)	Production date
THD59	290	350	10 - 12	2.100	4/19/95
THD60	325	425	7 - 9	2.098	4/19/95
THD58	360	500	2 - 3	2.038	4/19/95
THD61	400	575	< 1	1.930	4/19/95
THD82		475		2.400	12/18/95
THD83		504		1.950	12/18/95

Light induced degradation studies were performed on the series of hot-wire samples employing the photomixing technique to determine the dc photoconductivity σ_{dc}, lifetime τ and the drift mobility μ_d as a function of illumination time. The mixing and the light soaking were performed *in situ* employing a He-Ne laser with an intensity of 4 suns.

For intrinsic a-Si:H, the drift mobility is determined by the trapping of electrons into the conduction band tail and the scattering of electrons by the intrinsic (structural and/or electronic) disorder. Both enhanced trapping and scattering can result in the decay of the drift mobility. A question of interest is: which one is the dominant mechanism for the decay of the drift mobility upon light soaking. The concentration of defects generated by light soaking is usually about $(1-10)\times 10^{16}$ cm^{-3} for dangling bonds, located near the mid-gap, at saturation level[9] and about $10^{18} cm^{-3}$ for the light induced defects in the valence band tail[10]. Thus it is conceivable that

the conduction band tail (near the conduction band edge) would not be significantly altered by these defects, especially since the frequency dependent demarcation energy E_ω for the photomixing process is about 0.1 eV below the conduction band edge[2, 3] since the density of states for the conduction band tail is high (~10^{20}cm^{-3}eV^{-1}). Therefore the enhanced scattering has to be the dominant mechanism for the light induced decay of the drift mobility. In order for the light generated defects (~10^{18}cm^{-3}) to compete with the intrinsic neutral scatters (>10^{20} cm^{-3}) such as to reduce the drift mobility, part of the light generated defects need to be charged so that they can have much greater scattering cross sections and may form long-range potential fluctuations. Without significant changes for trapping, the lifetime τ and the drift mobility μ_d are thus proportional to the recombination lifetime τ_R and the extended state mobility μ_0. Therefore

$$\frac{1}{\tau} \propto \frac{1}{\tau_R} = N_r s_r v, \tag{3}$$

$$\frac{1}{\mu_d} \propto \frac{1}{\mu_0} \propto N_s s_s v, \tag{4}$$

where N_r, N_s are the effective concentrations of the recombination and the scattering centers, s_r, s_s are the effective recombination and scattering cross sections, and v is the thermal velocity of charge carriers.

Figs. 2-4 show the decay of the dc photoconductivity σ_{dc}, lifetime τ and the drift mobility μ_d as a function of illumination time for sample THD82 due to light soaking. Similar results were obtained on the other samples. The open dots are the experimental points while the solid lines are fitted to the following stretched exponential law:

$$N = N_s - (N_s - N_0)\, exp\,[-(t/\tau_0)^{\beta}], \tag{5}$$

by replacing N with $1/\sigma_{dc}$, $1/\tau$ and $1/\mu_d$ respectively, where N is the defect concentration at time t, N_0 and N_s are the initial and saturated defect concentrations, β is the stretching parameter, and τ_0 is the time constant.

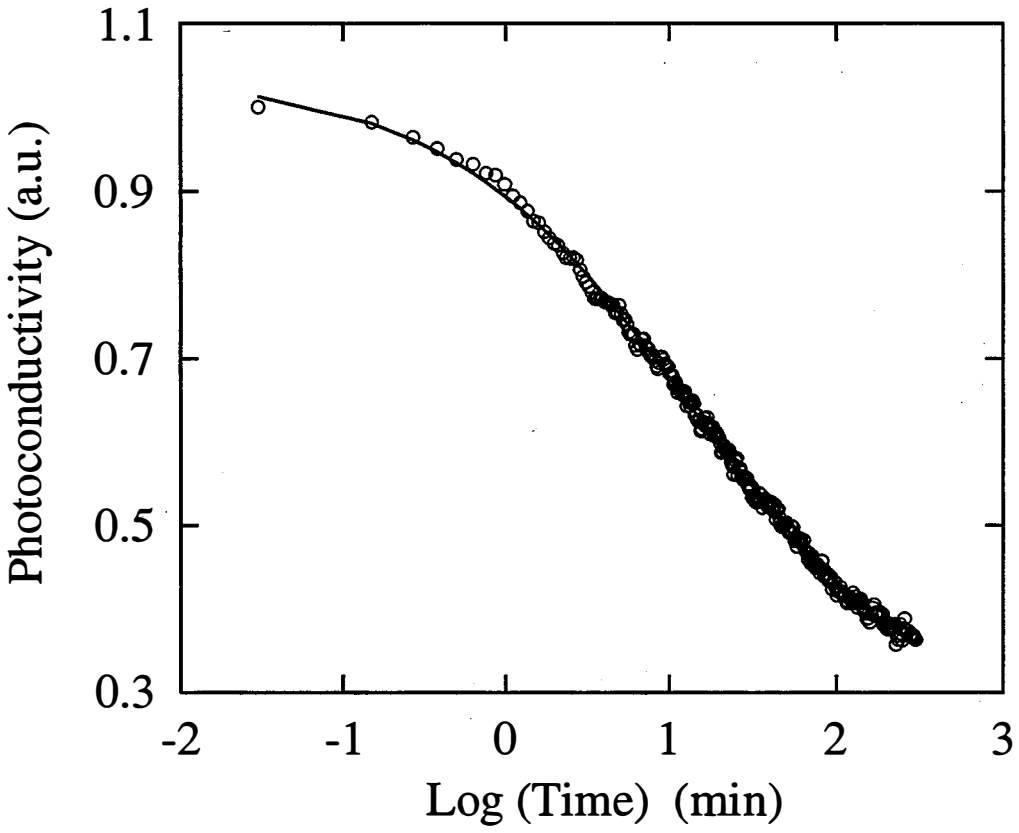

Figure 2. Photoconductivity decay vs. light soaking time for sample THD82.

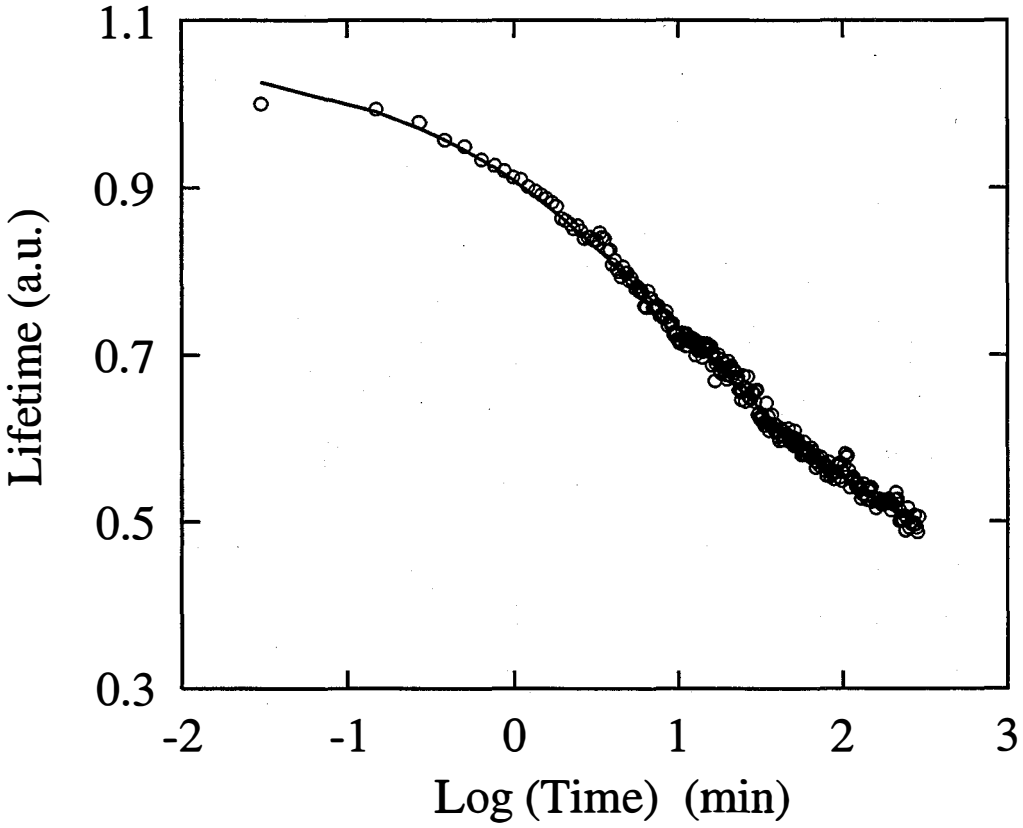

Figure 3. Lifetime decay vs. light soaking time for sample THD82.

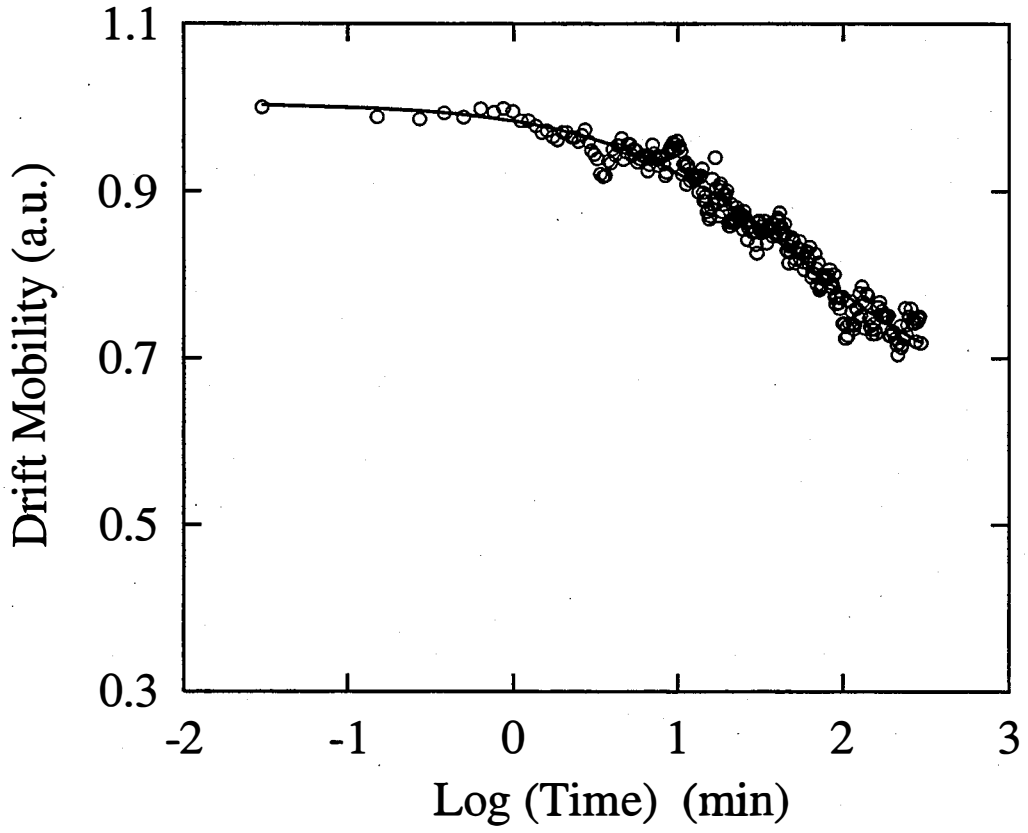

Figure 4. Drift mobility vs. light soaking time for sample THD82.

The results from curve fitting are listed in Table 2.

Table 2. Summary of results from the curve fitting of degradation measurement

sample ID	curve fitting from:	β	τ_0 (min)
THD59	photoconductivity	0.66	83
THD60	photoconductivity	0.64	75
THD58	photoconductivity	0.88	60
THD61	photoconductivity	0.77	76
THD82	photoconductivity	0.56	105
THD83	photoconductivity	0.63	174
THD59	drift mobility	0.51	23
THD60	drift mobility	0.49	36
THD58	drift mobility	0.88	70
THD61	drift mobility	0.72	76
THD82	drift mobility	0.66	95
THD83	drift mobility	0.67	297
THD59	lifetime	0.76	95
THD60	lifetime	0.64	74
THD58	lifetime	0.63	163
THD61	lifetime	0.62	105
THD82	lifetime	0.50	51
THD83	lifetime	0.67	258

As can be seen from the table 2, different stretched-exponential parameters for photoconductivity, lifetime and drift mobility were obtained, which indicates the generation of defects with different generation kinetics upon light soaking. Our studies so far do not reject any existing microscopic models[11, 12, 13-18] for the Staebler-Wronski effect, such as weak bond breaking [13-16] and charge trapping [17] models. Rather our studies indicate that combinations of different models may be necessary to explain the generation of defects with different characteristics. The recombination centers for electrons are most likely positively charged or neutral defects, whereas the scattering centers for electrons can be either negatively or positively charged defects. Upon light soaking, in addition to the generation of neutral defects, defects that serve as deep trapping or recombination centers are introduced. This results in enhanced scattering and thus the decay of the drift mobility for electrons. The charged defects may become quasi-stable through some relaxation processes and can also form certain long-range potential fluctuations[19-23], if they are not spatially correlated.

Temperature dependence measurements and Urbach Energy of intrinsic a-Si:H films

Extensive studies on effects of the deposition conditions, such as deposition temperature (T_s)[24-29] on the structural and electronic properties of these samples have been performed in attempt to improve the quality of these films for solar cell applications.

By measuring the dc and the ac photoconductivities at a single photomixing frequency as a function of temperature, the capture rate K, and the spread of the band tail ε can be determined by curve fitting the expression for the drift mobility μ_d derived in reference [4]. The relationship between drift mobility μ_d in the case of trapping and the extended state mobility μ_0 can be expressed as follows:

$$\mu_d = \mu_0 \frac{\omega}{\sqrt{\left[\omega + \frac{\pi}{2} kTKN_T(E_\omega)\right]^2 + [\varepsilon KN_T(E_\omega)]^2}}$$
$$= \mu_0 \frac{\omega}{\sqrt{\left[\omega/[KN_T(E_\omega)] + \frac{\pi}{2}kT\right]^2 + \varepsilon^2 K g_c}} exp\left(kT \frac{ln(N_c K/\omega)}{\varepsilon}\right) \quad (6)$$

where the distribution of tail states is given by: $N_T = g_c exp(-E/\varepsilon)$, and g_c is the density of states in the conduction band and ε is the spread of the band tail, $E_\omega = kTln(N_c K/\omega)$ is a frequency-dependent demarcation energy. N_c is the effective number of states in the extended state transport band, K is the capture rate.

Thus by measuring the ac photoconductivities at a single photomixing frequency as a function of temperature, K and ε can be determined through curve fitting according to above equation with assumed values for $N_c = 10^{20}$ cm^{-3} and $g_c = 10^{21}$ cm^{-3}.
Meanwhile the lifetime τ corresponding to μ_d can be written as

$$\tau = \frac{\mu_0 \tau_R}{\mu_d} = \frac{\sigma_{dc}}{eG_0 \mu_d}, \quad (7)$$

Where τ_R is recombination lifetime.

Figure 5 shows the dc photoconductivity as a function of temperature for THD 59 as an example. It should be noted that samples THD58-60 exhibit a plateau in the photoconductivity setting in around 200K, such behavior has been observed for low defect concentrations and is determined

by the recombination kinetics[30]. Figure 6 shows the temperature dependence of the drift mobility μ_d for THD59; the open circles are the experimental values while the smooth curves are curve fitted employing equation mentioned above. Similar results were obtained from the other samples (THD 58, 60, 61). The values of dc photoconductivity and drift mobility μ_d, as a function of the substrate temperature of the sample preparation, i.e. hydrogen concentration, are shown in Figures 7-8.(at 250 K) and the derived parameters ε and K as a function of the substrate temperature of the sample preparation, i.e. hydrogen concentration, are shown in Figures 9-10. (The nominal substrate temperatures are given in these figures, since we did not know the exact deposition temperatures.)

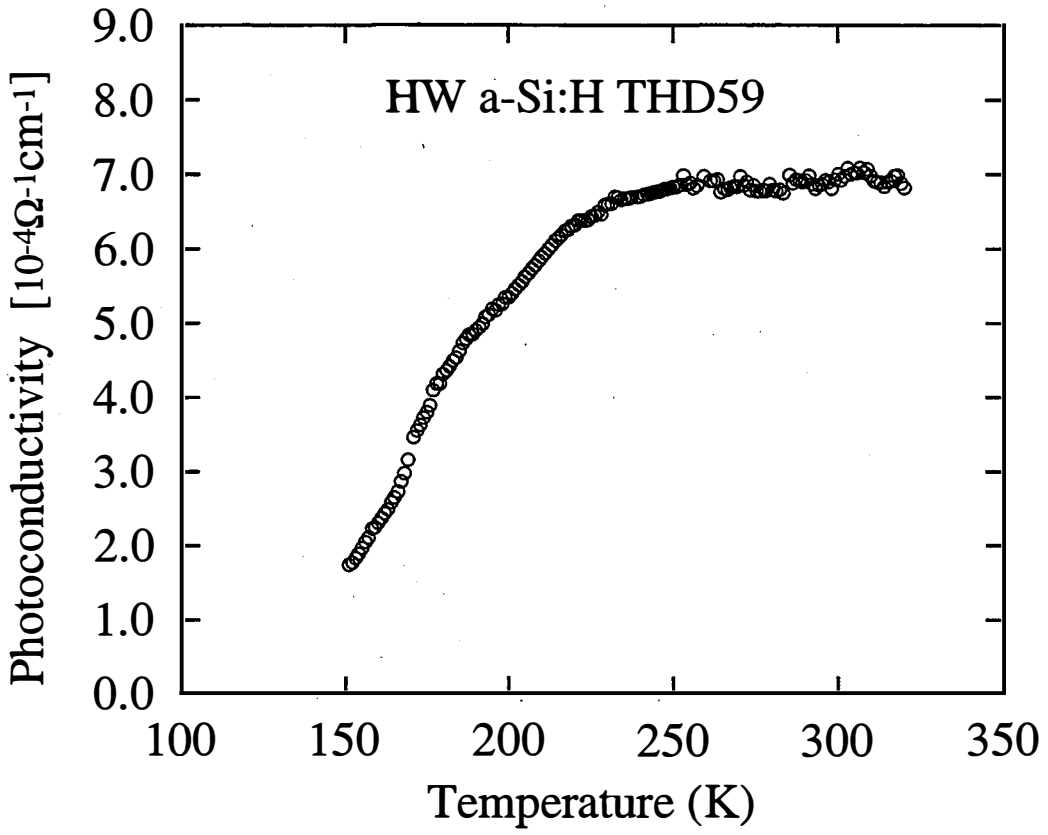

Figure 5. The dc photoconductivity as a function of measurement temperature for sample THD59.

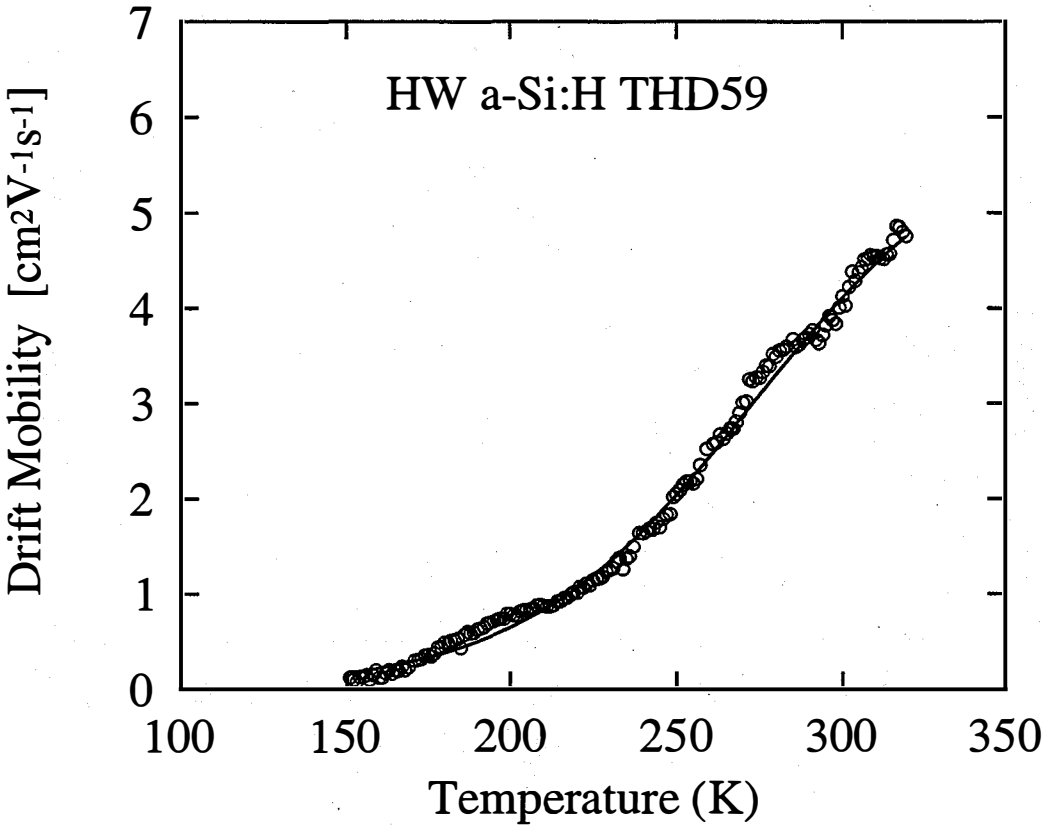

Figure 6. The drift mobility as a function of measurement temperature for sample THD59.

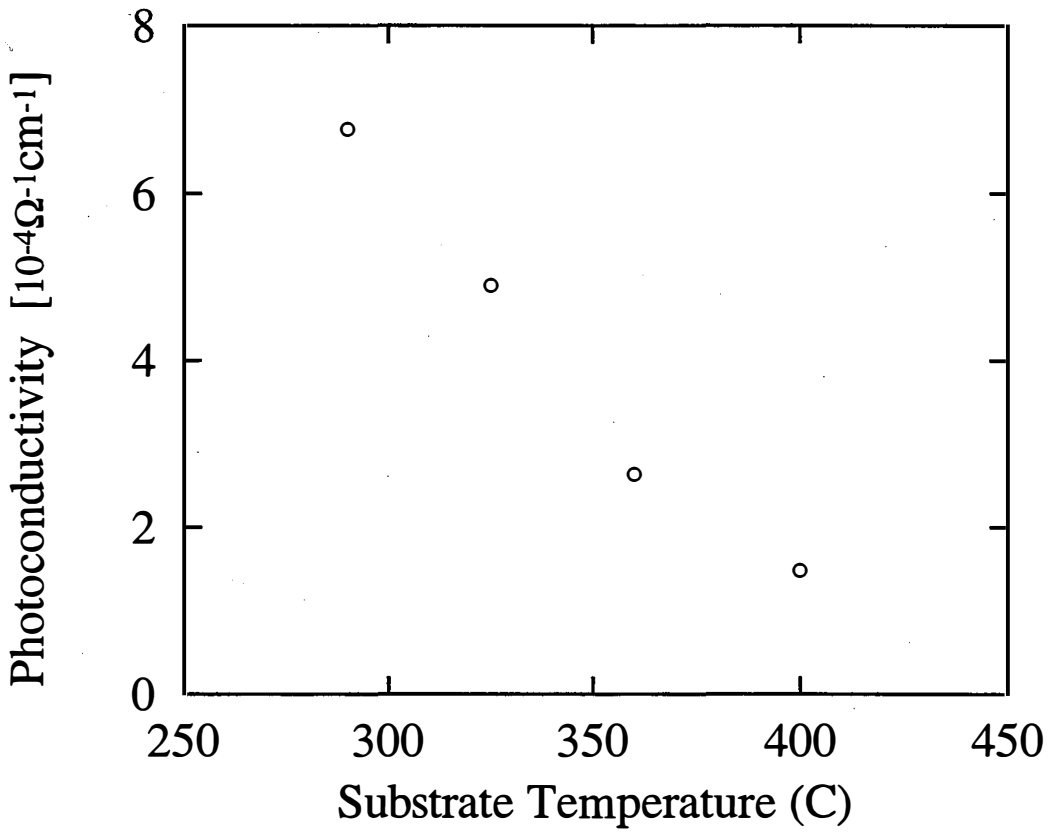

Figure 7. The photoconductivity as a function of the substrate temperature for the samples THD 58 - 61.

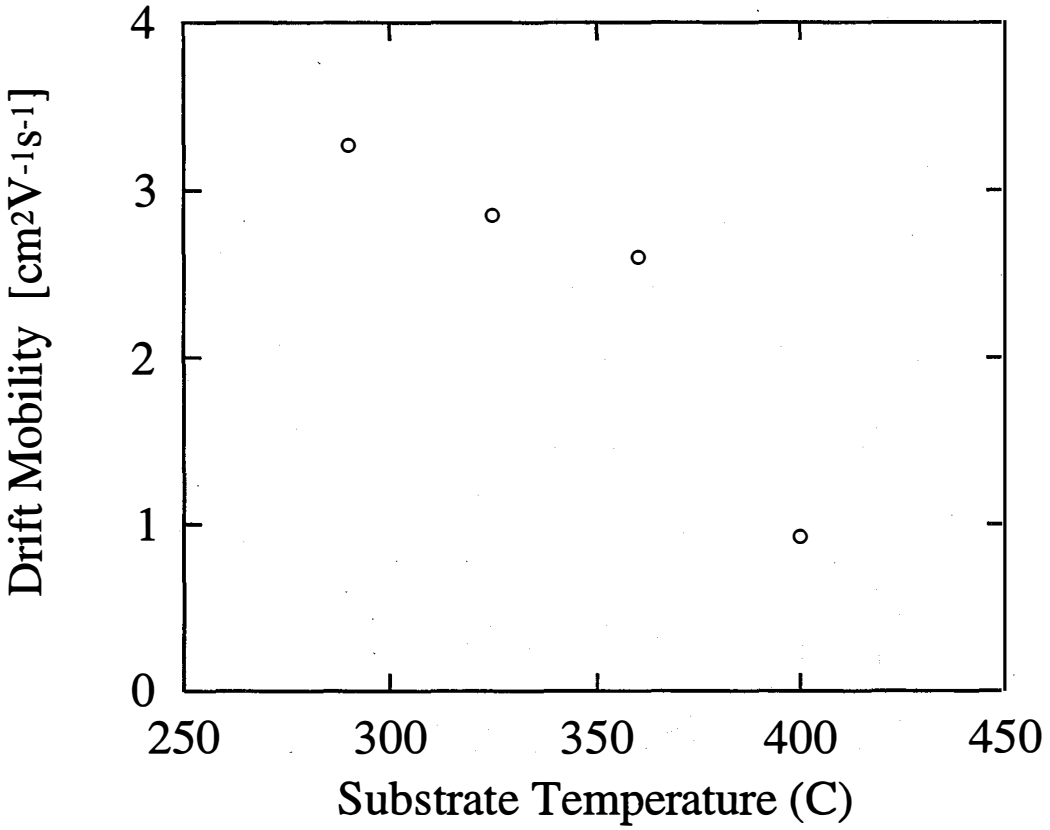

Figure 8. The drift mobility as a function of the substrate temperature for the samples THD 58 - 61.

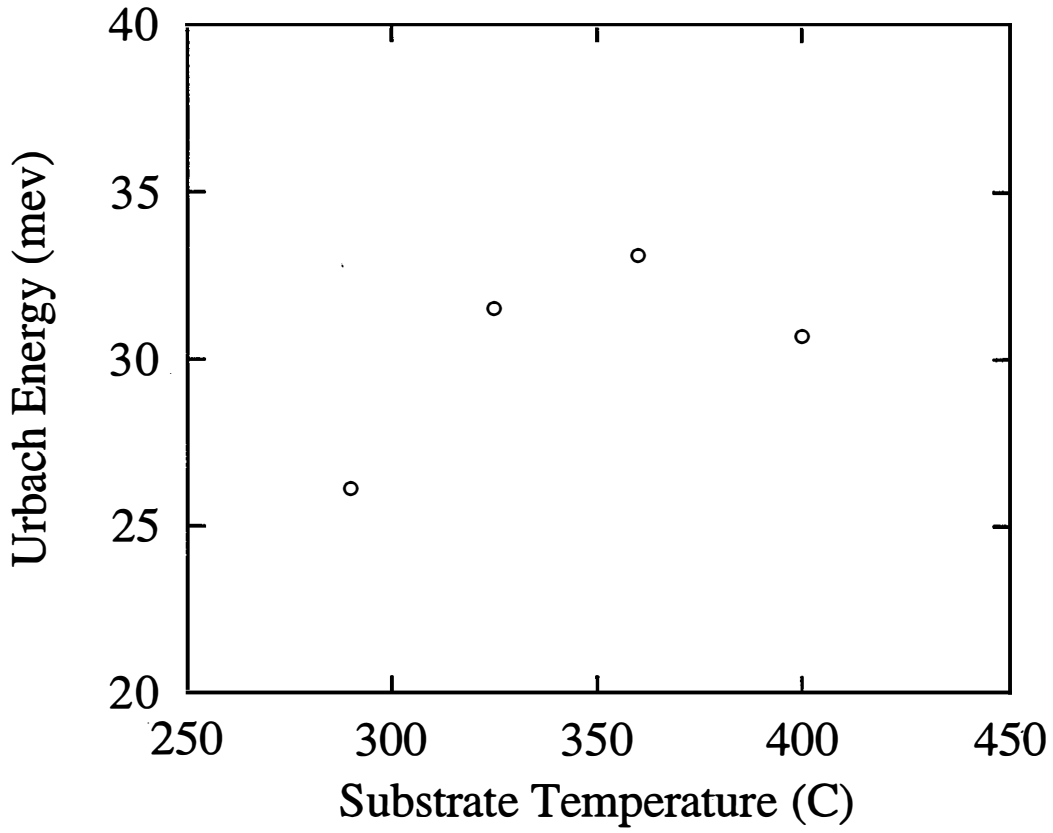

Figure 9. The Urbach energy as a function of the substrate temperature for the samples THD 58 - 61.

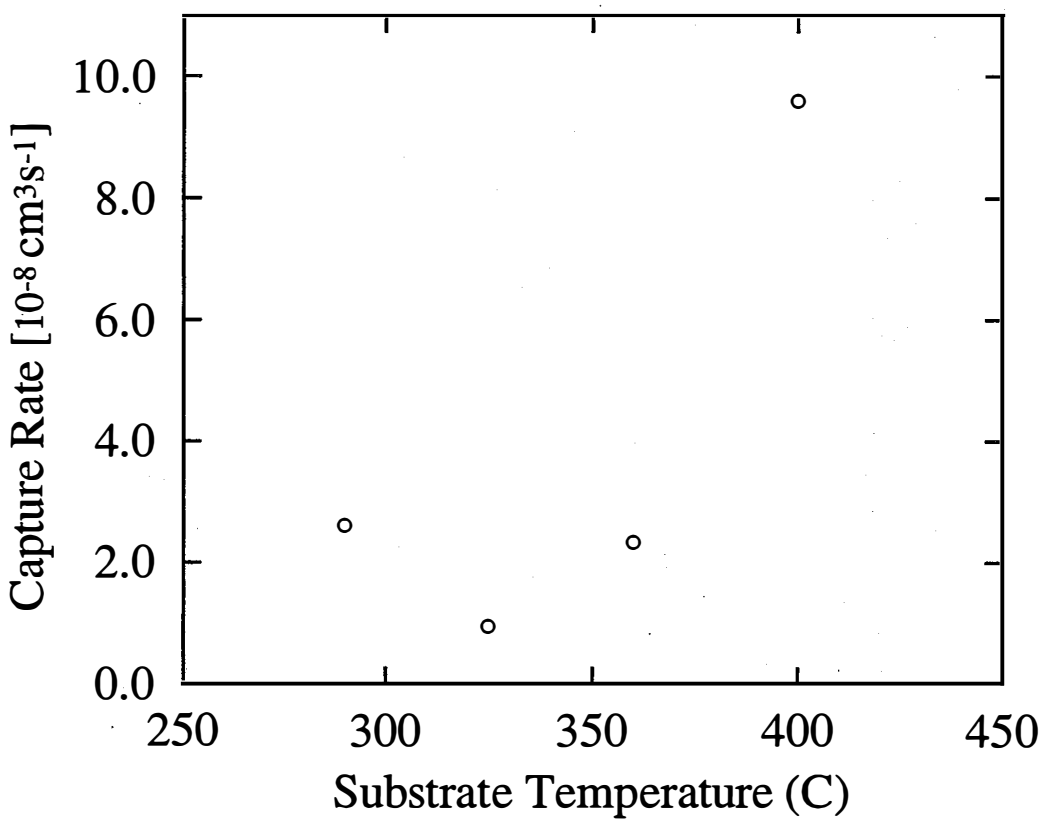

Figure 10. The capture rate as a function of the substrate temperature for the samples THD 58 - 61.

Because the hydrogen content of hot-wire a-Si:H films increase with the deceasing deposition (or substrate temperature), both of dc photoconductivity and drift mobility decease with the deceasing of the hydrogen content as expected, while, the Urbach energy increases with the deceasing of the hydrogen content, which is predicted by the equation 6. An exception seems to be the sample THD61.

Mobility and lifetime in as-grown, annealed and light soaked conditions in hot-wire intrinsic a-Si:H

We have utilized the capabilities of our photomixing technique to separately determine the mobility and lifetime under as-grown, annealed and under light soaked conditions on these samples. The samples THD58 - 61 were produced at NREL on 4/19/95 and the samples THD82 - 83 were produced on 12/18/95 by Brent Nelson and Eugene Iwaniczko. Samples were prepared in a special "Hot Wire"deposition chamber attached to the doping section of NREL's "T" deposition system. It might thus be possible that different trace amounts of dopants could be present in the two sets of samples. Our goal was to characterize such samples by our techniques and gain insight into the factors which determine the properties of these films.

After light soaking for 5 hours at 4 sun intensity, all samples were annealed at 150 ^{o} C for one hour and cooled down to room temperature, whose characteristics are given in table 3 and table 4. where the drift mobility, lifetime and dc photoconductivity (σ_{dc}) are shown for given field (6050 V/cm) for the as-grown, annealed state and light soaked state.

For samples THD82-83, the values of σ_{dc} are almost the same both in the annealed and as-grown states, but the magnitude of μ_d tends to decrease, meanwhile the magnitude of τ tends to increase in the annealing process.(see table 3) As a comparison, another batch of samples, THD58-61, show different behavior, as we reported early. (see table 4). The values of the drift mobility in the annealed state obviously are much larger than that in the as-grown state, meanwhile, the lifetime become smaller as compared with that in the as-grown state. It indicate that the concentration or nature of the defects in the as-grown and in the annealed states could be different which depend on the process of production.

Table 3. μ_d, τ and σ_{dc} for THD82-83 in all states (produced on 12/18/95)

Sample ID	Substrate Temp.(C)	State	μ_d $cm^2V^{-1}s^{-1}$	τ ns	σ_{dc} $10^{-4}\Omega^{-1}cm^{-1}$
THD82	475	as grown	2.06	47.1	2.8
THD83	504	as grown	1.79	34.7	2.2
THD82	475	annealed	1.98	56.2	3.25

Table 3. μ_d, τ and σ_{dc} for THD82-83 in all states (produced on 12/18/95)

Sample ID	Substrate Temp.(C)	State	μ_d $cm^2V^{-1}\ s^{-1}$	τ ns	σ_{dc} $10^{-4}\Omega^{-1}cm^{-1}$
THD83	504	annealed	1.51	46.1	2.51
THD82	475	l.s.	0.89	41.1	1.07
THD83	504	l.s	1.3	27,4	1.27

Table 4. μ_d, τ and σ_{dc} for THD58,60 and 61 in all states. (produced on 4/19/95)

Sample ID	Substrate Temp.(C)	State	μ_d $cm^2V^{-1}\ s^{-1}$	τ ns	σ_{dc} $10^{-4}\Omega^{-1}cm^{-1}$
THD60	425	as grown	1.85	103.9	6.1
THD58	500	as grown	1.61	49.9	2.9
THD61	575	as grown	0.81	67.2	2.0
THD60	425	annealed	2.23	78.3	5.8
THD58	500	annealed	2.3	41.9	3.0
THD61	575	annealed	1.11	45.7	1.7
THD60	425	l.s	1.62	36.4	2.0
THD58	500	l.s	1.36	30.5	1.5
THD61	575	l.s	0.84	43.8	1.3

Electric field dependence of mobility in hot-wire intrinsic a-Si:H films

The electric field dependence of the drift mobilities (μ_d) and the lifetimes (τ) of these samples were measured in the as-grown state, the annealed state (1hours at 150 C) and in the light soaked state (5 hours at 4 sun intensity). It was found that the drift mobility (μ_d) increases with increasing electric field, while the lifetime (τ) decreases with increasing electric field, and the $\mu\tau$ product is essentially independent of the electric field in the range from 1,000 V/cm to 10,000 V/cm. The fact that the lifetime decreases while the drift mobility increases indicates the existence of the diffusion limited transport and recombination[31] in all the samples in the light soaked as well as the as grown and the annealed states. It should be pointed out that in this case, the increase in μ_d with increasing field as well as the increasing in μ_d with increasing carrier density due to light illumination, can possibly be explained by the existence of long-range potential fluctuations[32-39]. The increase in μ_d is compensated by the corresponding decrease in τ, which can result in a field

independent $\mu\tau$ or the commonly observed ohmic behavior of the photocurrent. In the presence of long range potential fluctuations, one would expect μ to increase with increasing electric field and with increasing carrier concentration[5, 40, 41]. Such increase in the drift mobility do not necessarily lead to an increase in the photoconductivity, since one commonly observes a corresponding decrease in τ.

Figures 11-16 show the electric field dependence of the drift mobility for samples THD58-61 andTHD82-83 respectively. The solid diamonds, open dots and solid dots are the experimental points for the annealed, the as-grown and light soaked state respectively. The solid curves were obtained by a curve fitting procedure to a model of transport through potential barriers which we presented in the paper we published[5].

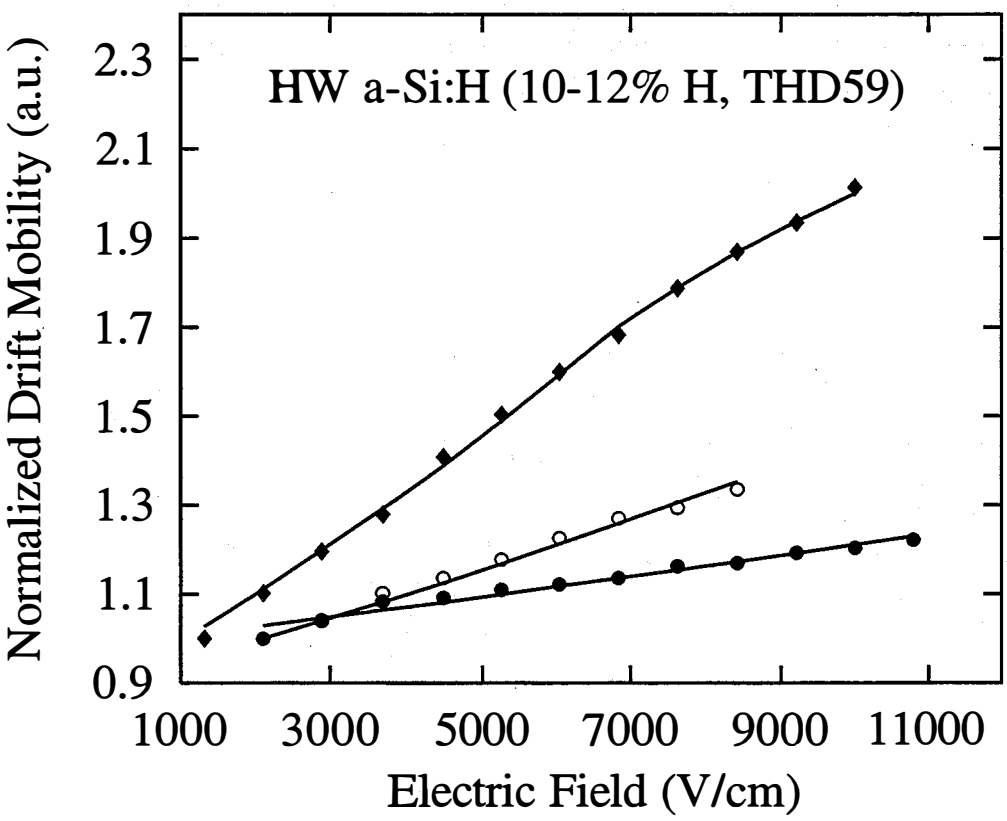

Figure 11. The normalized drift mobility versus electric field for sample THD59.

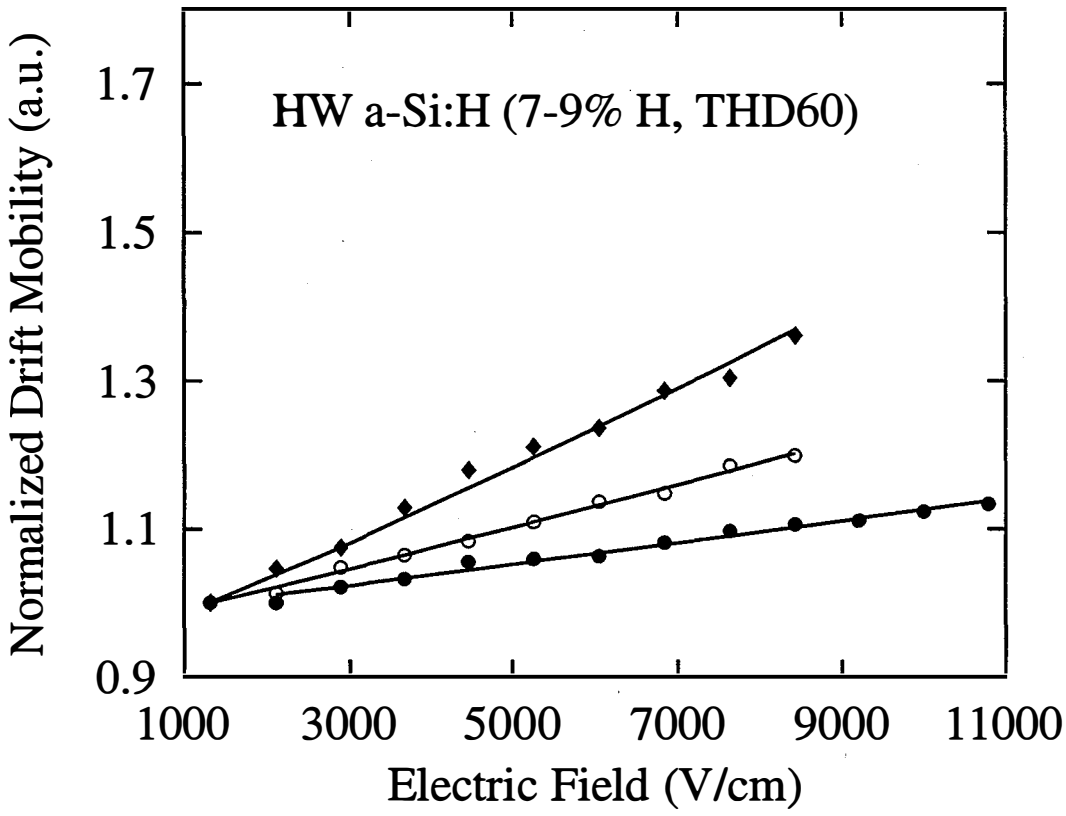

Figure 12. The normalized drift mobility versus electric field for sample THD60.

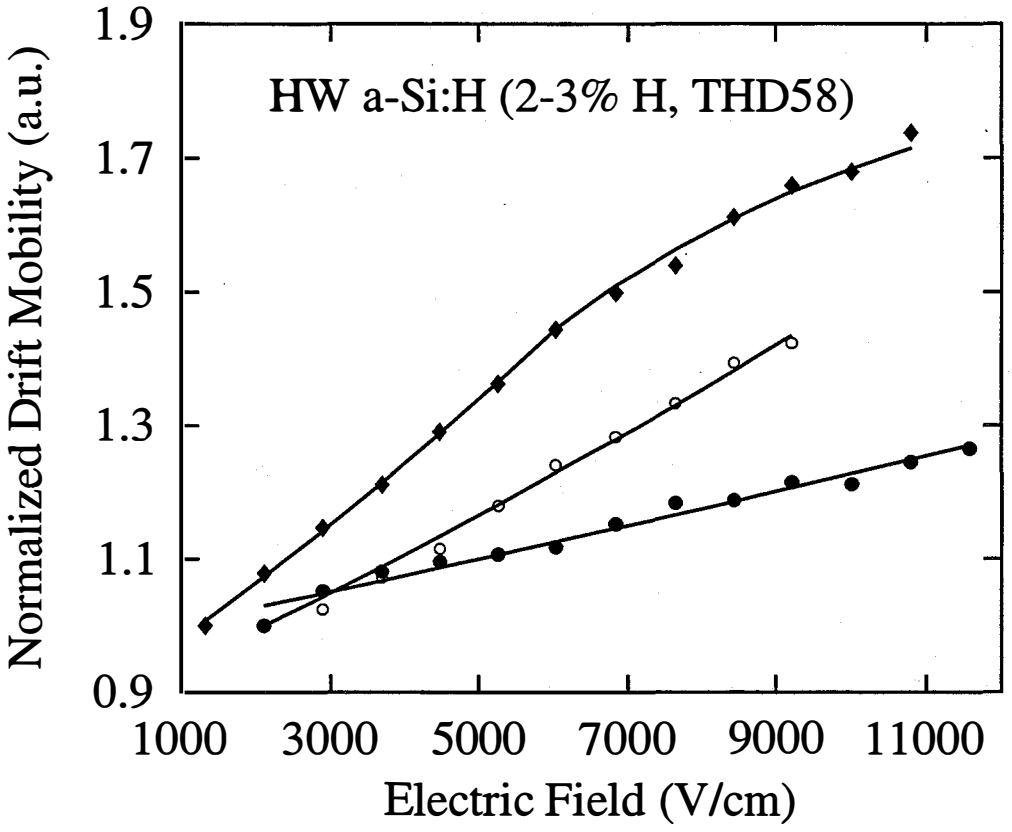

Figure 13. The normalized drift mobility versus electric field for sample THD58.

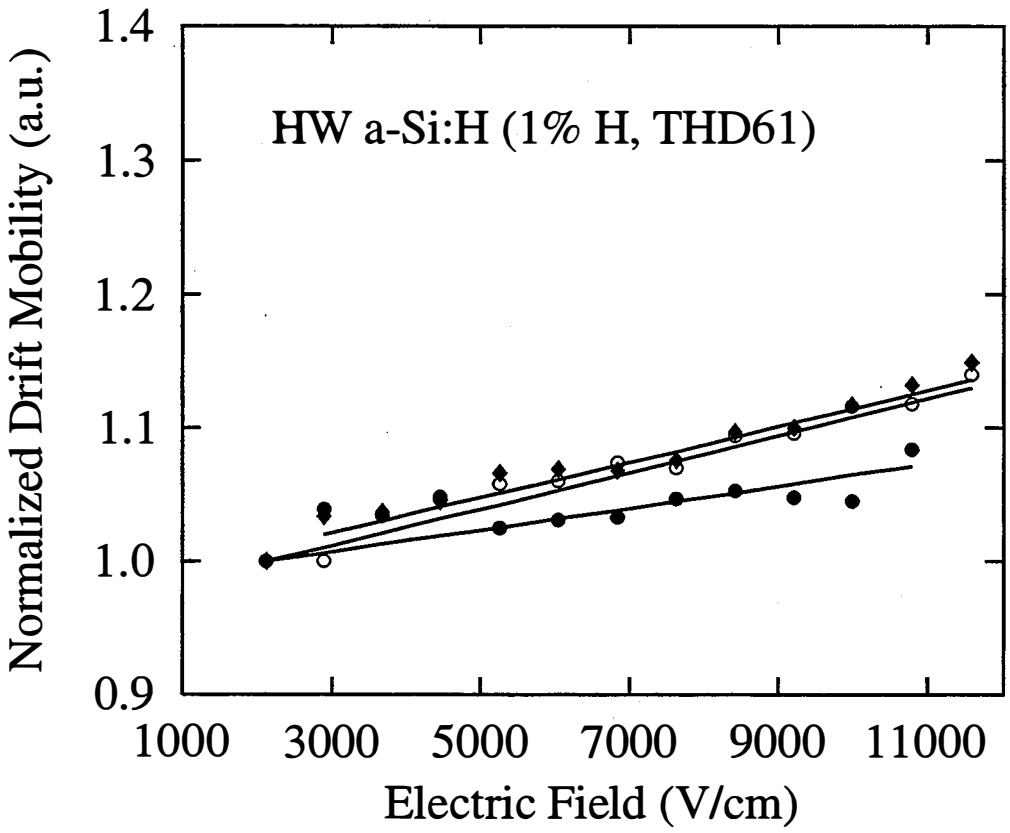

Figure 14. The normalized drift mobility versus electric field for sample THD61.

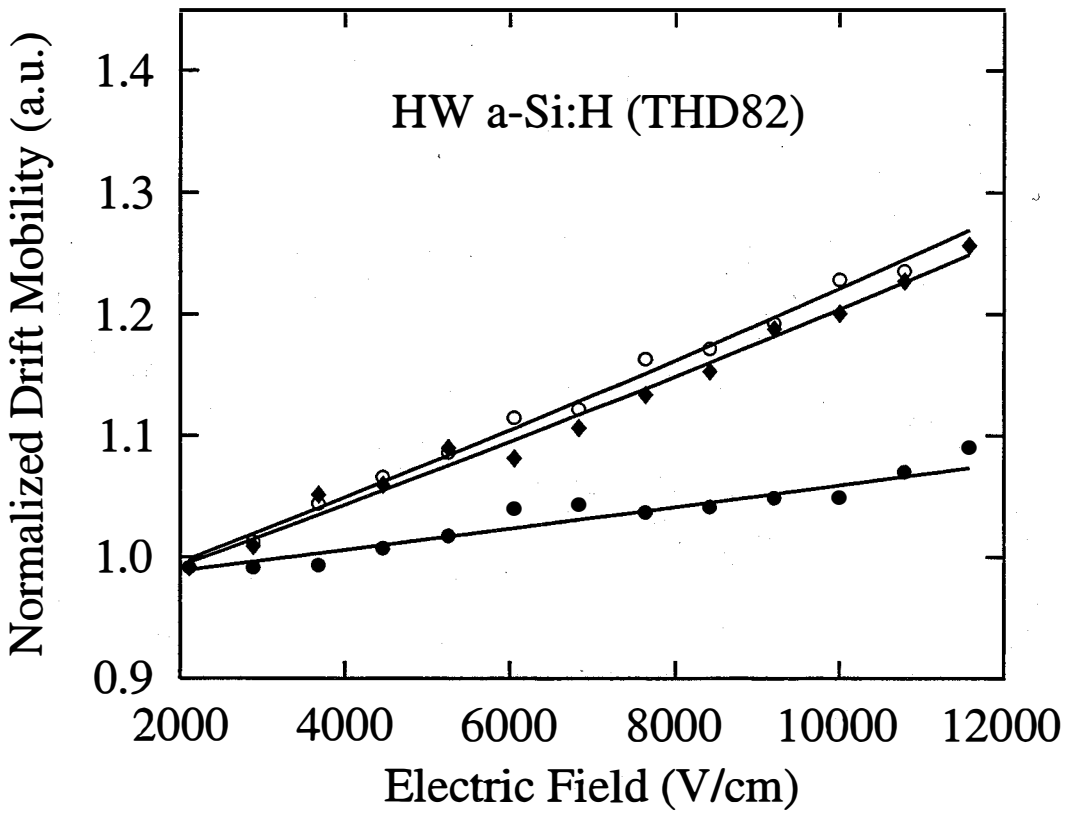

Figure 15. The normalized drift mobility versus electric field for sample THD82.

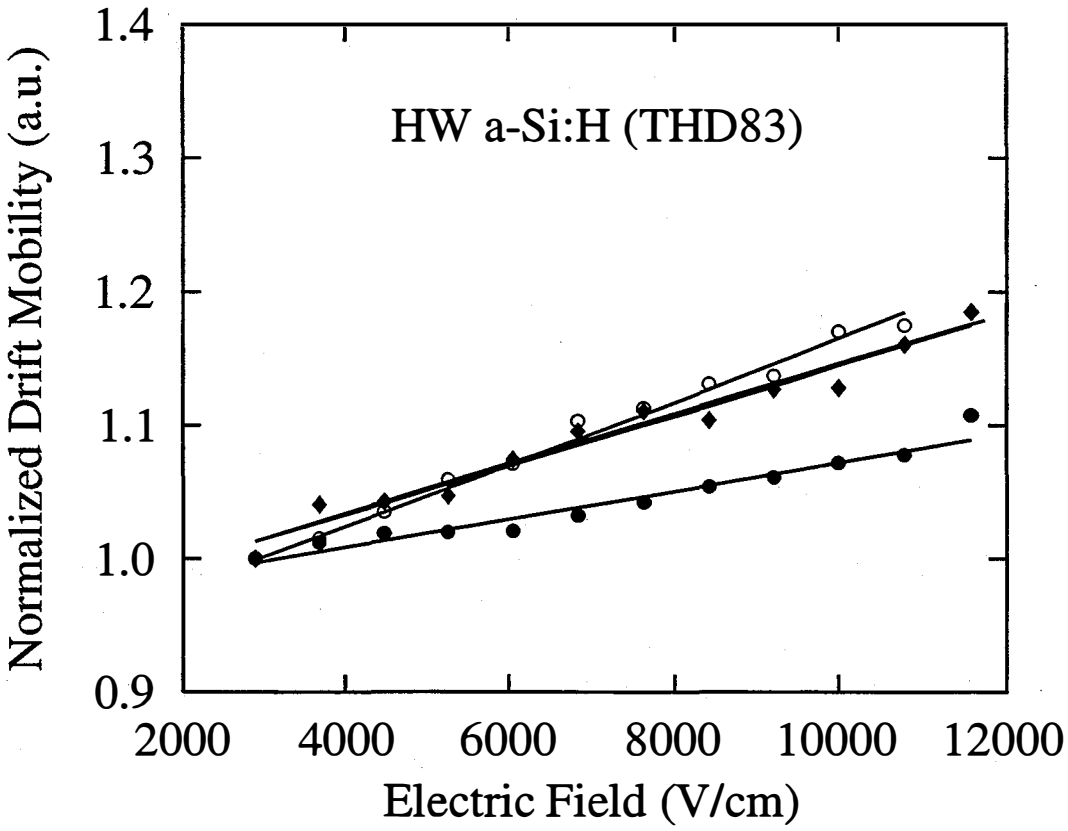

Figure 16. The normalized drift mobility versus electric field for sample THD83.

The results in Fig. 11- 16 agree with our observation that light soaking decreases the magnitude of μ_d.The light induced defects as well as the native defects, which serve as recombination centers and trapping centers, can be charged and can form certain potential barriers or fluctuations. In the transport process, the charged carriers can either go over the potential barrier through thermal activation or go around the potential barrier through scattering. If the former dominates the latter, then through simple statistical calculations one can obtain the following electric field (E) dependence of the drift mobility $\mu_d(E)$:

$$\mu_d(E) = \mu_d^0 \exp\left(-\frac{eV_P}{kT}\right)\frac{eLE}{kT\left[1-\exp\left(-\frac{eLE}{kT}\right)\right]} \qquad (if\ |LE| \le V_P)$$

$$\mu_d(E) = \mu_d^0 \frac{\exp\left(-\frac{eV_P}{kT}\right)}{\frac{kT}{eLE}+\left(1-\frac{V_P}{LE}-\frac{kT}{eLE}\right)\exp\left(-\frac{eV_P}{kT}\right)} \qquad (if\ |LE| > V_P)\ , \qquad (8)$$

where μ_d^0 is the drift mobility without the potential fluctuations, while Vp and L are an average magnitude and range of the potential fluctuations, respectively.

During the light soaking process, the magnitude (V_P) of the potential fluctuations has a tendency to increase, whereas the range (L) of the potential fluctuations has a tendency to decrease. But because of the long range nature of the potential fluctuations, the potential fluctuations should be spatially nondegenerate. Therefore, during the light soaking process, the magnitude (V_P) of the potential fluctuations should not increase as significantly as the range (L) of the potential fluctuations decreases. This is partially evidenced by the experimental results that the field dependence of the drift mobility is less in the light soaked state than that in the annealed state.

It is reasonable to assume that the charged defects are responsible for the long-range potential fluctuations. In a-Si:H, a reasonable candidate for the charged defects is the charged dangling band state ($T_3^{+/-}$). Just as in the case of neutral dandling bonds (T_3^0), a fraction of the charged dangling bonds ($T_3^{+/-}$) is stable, while another fraction in metastable, i.e., the density of the latter increases upon light soaking and decreases upon annealing. The existence of the stable and metastable charged dangling bonds ($T_3^{+/-}$) has been attributed to the local dipole potential fluctuations[35]. In the context of this report, it is not important to differentiate whether a $T_3^{+/-}$ defect is newly created or it is converted from a T_3^0 defect. Assuming that the density (n) of the $T_3^{+/-}$ defects is determined by[37,38]:

$$n \propto V_P^2/L, \qquad (9)$$

we can estimate the lower limit of the ratio of the defect densities in the light soaked state (n_{LS}) and that in the annealed state (n_{AN}) can be estimated by $n_{LS}/n_{AN} = L_{AN}/L_{LS}$, where L_{AN} and L_{LS} are the ranges of the potential fluctuations in the annealed and light soaked states, respectively. The results of such ratios are also included in Table 5.

It should be pointed out that our results suggest that the light induced charged dangling bonds may not affect $\mu\tau$ by increased recombination, but rather by affecting μ_d through controlling potential fluctuations in the sample. It has been found that upon light soaking both τ and μ_d decease following different stretched exponential law.[4] Stretched exponential behavior is typical for hierachically constrained systems, and transport phenomena appear to provide a barrier or constraint for degradation phenomena.[42]

Table 5. Range of the potential fluctuations

Sample ID	L (Å) As-grown	L (Å) Annealed	L (Å) Light soaked
THD59	278	569	115
THD60	144	207	74
THD58	310	445	125
THD61	80	95	41
THD82	152	143	49
THD83	118	94	54

Photomixing measurement on solar cell devices

Photomixing measurement have been performed on two Schottky structure samples fashioned on PEVCD (TPni48) and hot-wire (THDni50) films respectively from NREL (Crandall, Mahan, Nelson). A neutral density filter was used to reduce the light intensity of the He-Ne laser. Golden spring contact was used for the electric contact. The dc dark current, dc photocurrent and mixing power versus reverse bias were measured.

Figures 17 and 18 show reverse bias dark I-V data for TPni48 and THDni50 respectively. Open circles are experimental data, solid line is a fitting curve according the empirical diode equation[43]:

$$I = I_0 \exp\left(qV/(nkT)\right)\left(1 - \exp\left(-qV/(kT)\right)\right), \qquad (10)$$

Where n is the ideality factor. A semilog plot of I/(1-exp(-qV/(kT)) versus reverse bias is a linear relation and the factor n can be obtained from the slope. The n value is 1.02 for both of these two samples.

Figures 19 and 20 shows dc photocurrent versus reverse bias for TPni48 and THDni50 respectively. Open circles are experimental data. The solid line is fitting curve employing the equation[44]:

$$J = qF\left(1 - \exp(-aW)/\left(1 + aL_p\right)\right) + (qP_0D_p)/D_p, \tag{11}$$

where a: the absorption coefficient.
W: the thickness of the depletion layer.
L_P: diffusion length.
P_0: the equilibrium hole density.
D_p: the diffusion coefficient for holes.
F: the incident photon flux.

aW and aL_P can be obtained from curve fitting. When the voltage across the depletion layer is 1 volt for sample TPni48, aW and aL_P are 2.52 and 0.01 respectively. For sample THD50 aW and aL_P are 0.48 and 0.076 respectively.

Figures 21 and 22 are the square root of mixing power as a function of reverse bias. Open circles are experimental data. The solid line is fitting curve using modified Gartner's formula; Gartner discussed the transit time effects at high modulation frequencies and proposed a formula to describe the ac current vs. voltage relationship which assume all series resistances and capacitances to be negligible. We suppose that the square root of mixing power is proportional to the ac photocurrent, and assume that there is not only a surface generation. The ac photo current may be expressed as in the following equation:

$$I_{ac} \propto j\frac{\varepsilon\omega V_D}{W} + q\Phi\left(\frac{1-\exp(-j\omega t_0)}{j\omega t_0} - \frac{1-\exp(-aW)\exp(-j\omega t_0)}{aW + j\omega t_0}\right), \tag{12}$$

where ε is the dielectric constant, ω is the mixing (or modulation) frequency, V_D the voltage across the depletion layer, t_0 is the transit time of carriers through the depletion layer.

The transit time of carriers through the depletion layer t_0 can be obtained from above curve fitting. They are 1.6×10^{-8} sec. and 2.3×10^{-8} sec. for TPni48 and THDni50 respectively.

We plan to measure the light induced degradation and illumination intensity dependence of the dc and ac photocurrent, if we can get more Schottky samples, because the Schottky barrier junctions were shunted easily as our measurements were carried out.

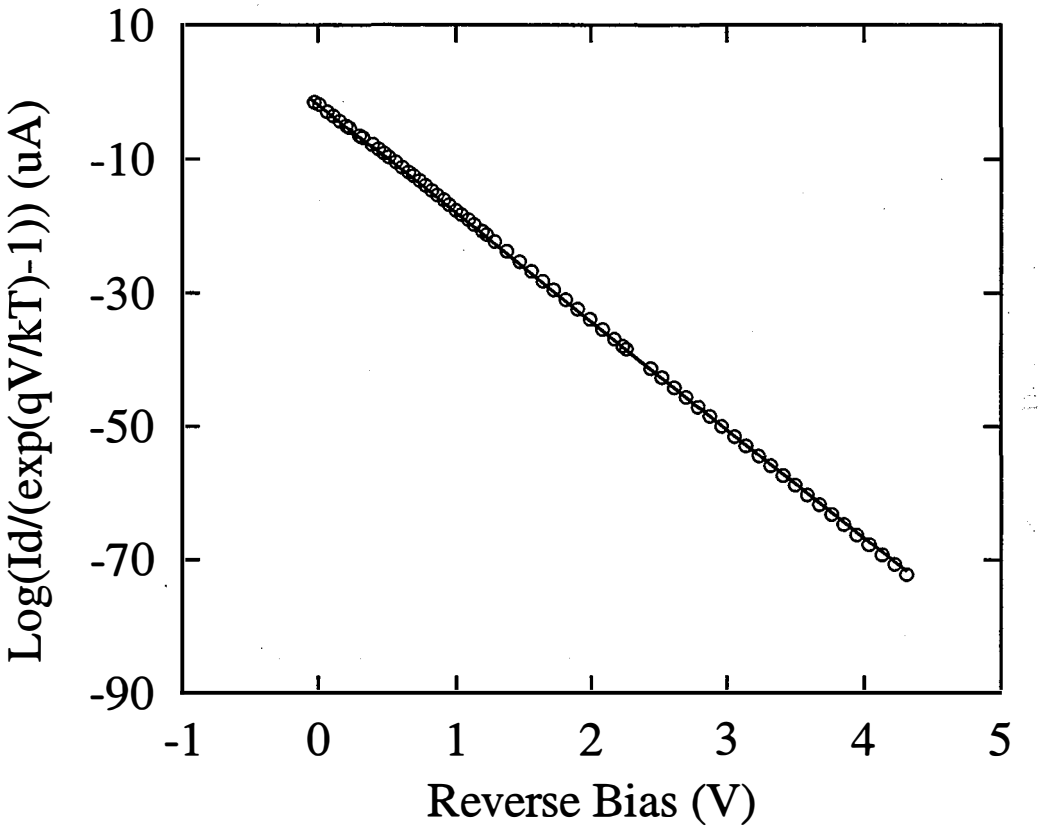

Figure 17. The dark current vs. reverse bias for Schottky sample

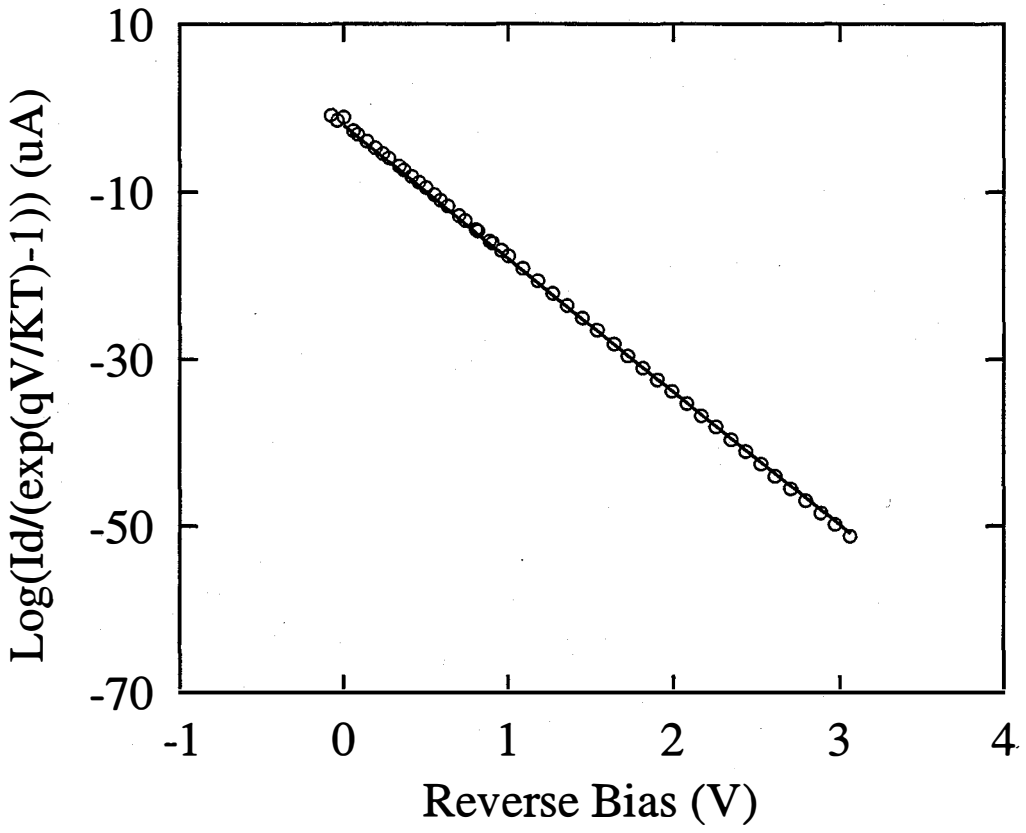

Figure 18. The dark current vs. reverse bias for Schottky sample THDni50.

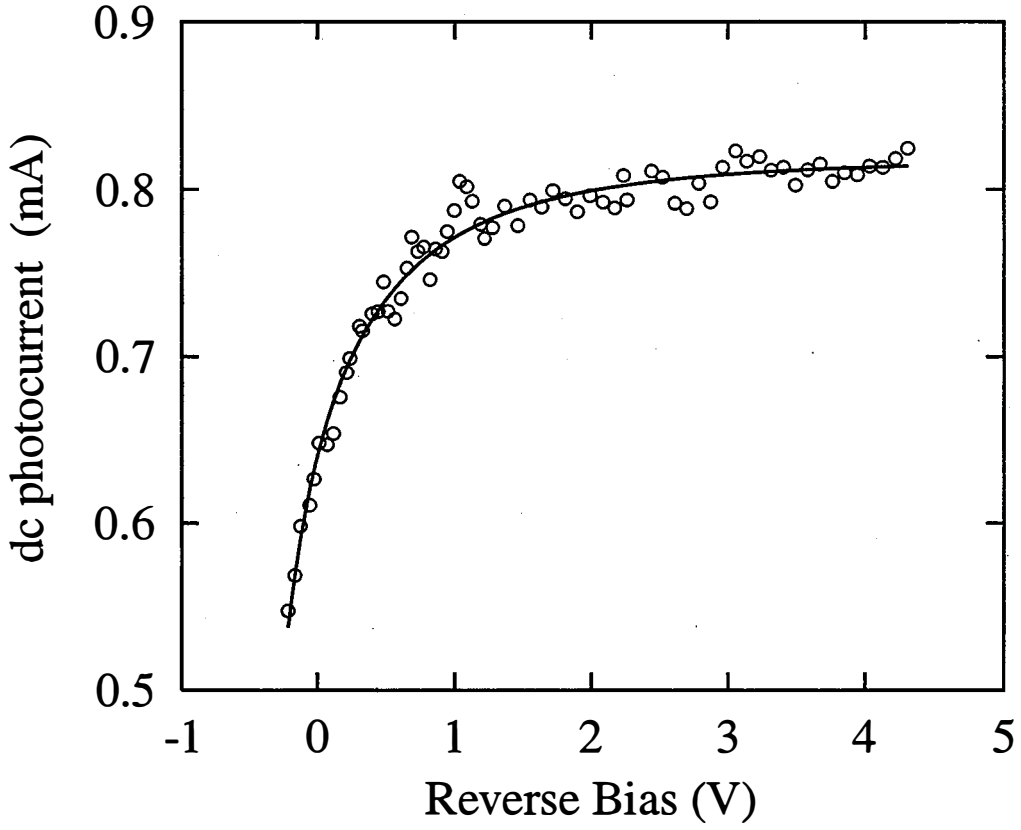

Figure 19. The dc photo current vs. reverse bias for Schottky sample TPni48.

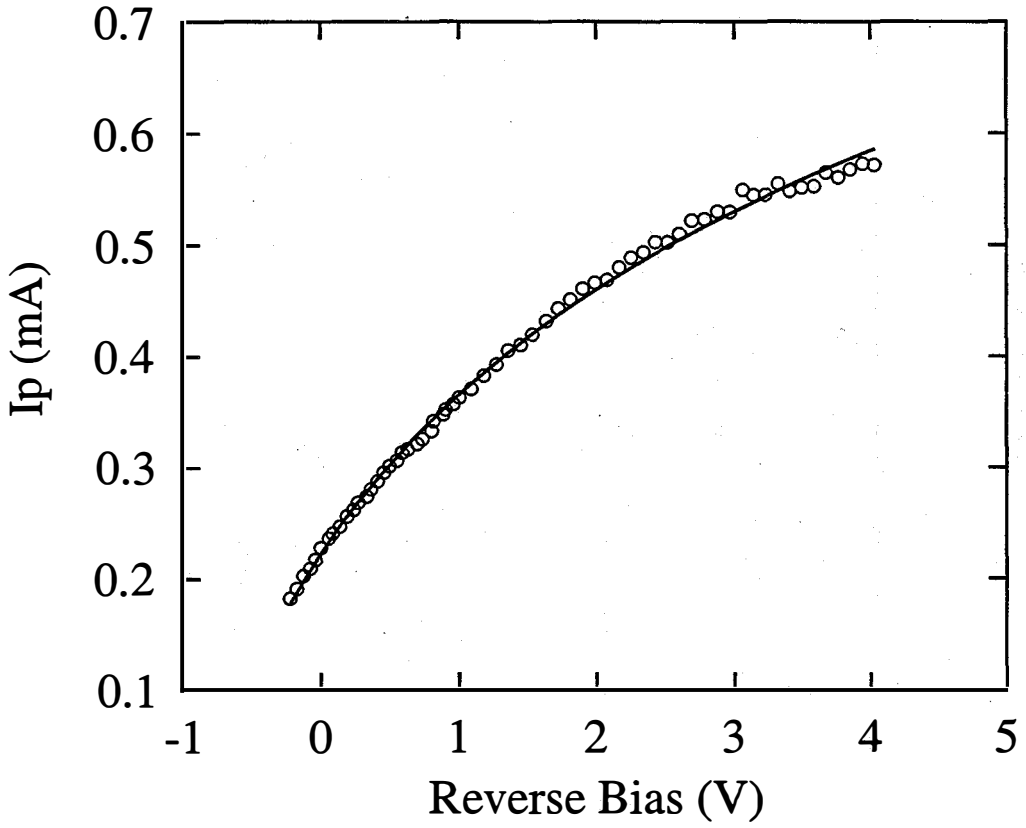

Figure 20. The dc photocurrent vs. reverse bias for Schottky sample THDni50.

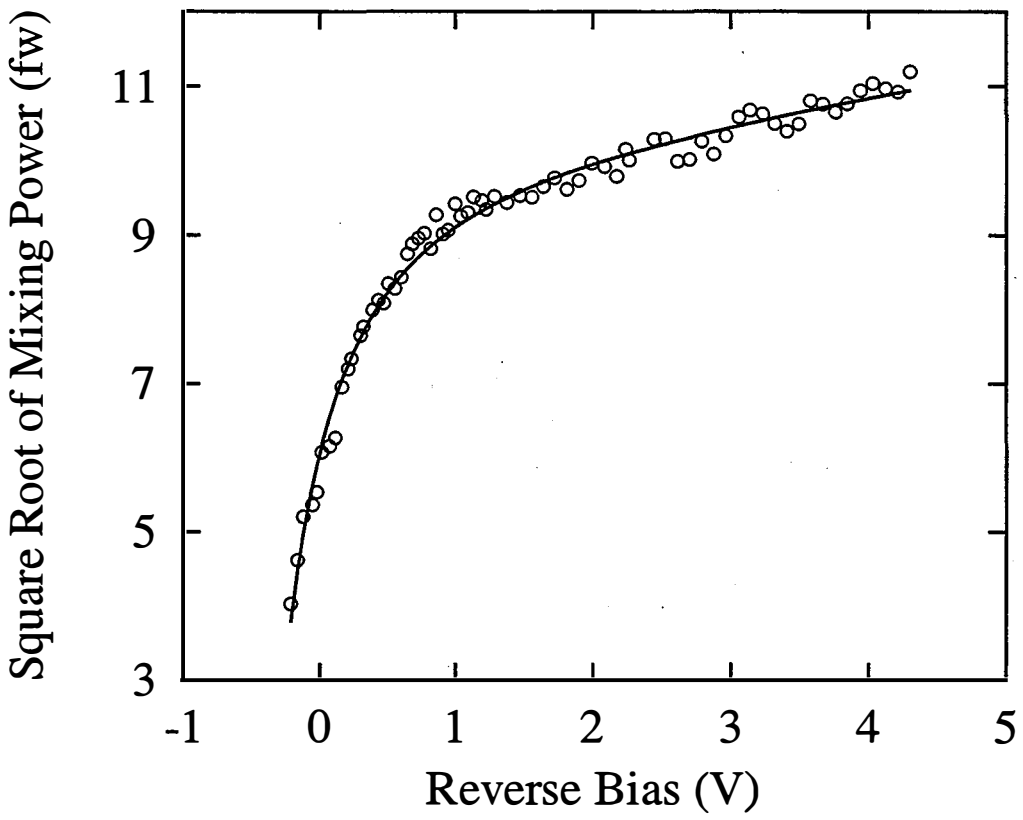

Figure 21. The mixing power vs. reverse bias for Schottky sample TPni48.

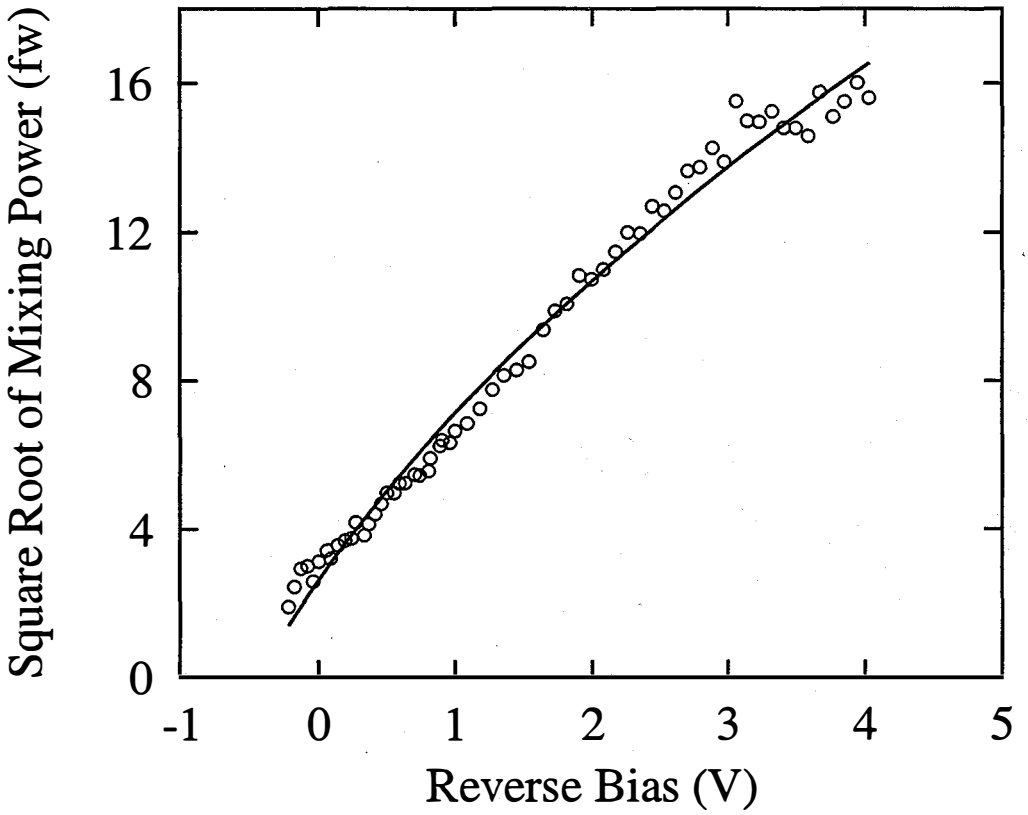

Figure 22. The mixing power vs. reverse bias for Schottky sample THDni50.

Abstract

The transport properties of intrinsic hydrogenated amorphous silicon samples with the hydrogen content ranging from over 10% to less 1%, which were produced by hot-wire technique at NREL, were systematically studied by the photomixing technique. The effects of deposition conditions on transport properties were investigated as a function of substrate temperature ($290C \leq T_s \leq 400C$). It was found that with increasing substrate temperature, the lifetime, the drift mobility and the photoconductivity decreased but the Urbach energy (~ 0.1 eV below the conduction band) increased. These results indicate that for the a-Si:H films with increasing deposition temperature, the density of positively charged, negatively charged, and neutral defects all show a tendency to increase in agreement with the results observed by other workers employing other measurement techniques. The continuous degradation of photoconductivity, lifetime and drift mobility were found during light soaking which obey different stretched-exponential laws which indicates the production of defects with different generation kinetics upon light soaking.It was found that the drift mobility (μ_d) of these samples increases, the lifetime (τ) decreases with increasing electric field, while the $\mu\tau$ product is essentially independent of the electric field in the range of 1000 V/cm - 10,000V/cm. The electric field dependence of mobility $(\Delta\mu)/\mu_0/(\Delta E)$ in the as-grown or/and annealed states are always larger than that in the light soaked state. This electric field dependence of mobility can be explained by the existence of long-range potential fluctuations. Employing a model for potential fluctuations, whose range can be determined employing a model which we have developed.

Preliminary photomixing measurements were performed on Schottky structure, from which such parameters as the products of the thickness of depletion layer and absorption coefficient, barrier potential and transit time were obtained.

References

1. 1. E. R. Giessinger, R. Braunstein, S. Dong, and B. G. Martin, *J. Appl. Phys.* **69**, 1469 (1991).

2. Yi Tang, R. Braunstein, and B. von Roedern, *Mat. Res. Soc. Symp. Proc.* **258**, 735 (1992).

3. Yi Tang, R. Braunstein, B. von Roedern, and F. R. Shapiro, *Mat. Res. Soc. Symp. Proc.* **297**, 407 (1993).

4. Yi Tang, R. Braunstein, *J. Appl. Phys.* **79**, 850 (1996).

5. Yi Tang, S. Dong, R. Braunstein and B. von Roedern, *Appl. Phys. Lett.* **68**, 640 (1996).

6. R. Braunstein and Yi Tang, *Proceedings of the 21st International Conference on Physics of Semiconductors* (August 1992), Beijing, China, **1**, 269.

7. Yi Tang, R. Braunstein, and B. von Roedern, *Appl. Phys. Lett.* **63** (17), 2393 (1993).

8. A. H. Mahan, J. Carapella, B.P. Nelson, R. S. Crandall and I. Baberg,*J. Appl. Phys.* **69**, 6728 (1991)

9. M. Stutzmann, W. B. Jackson, and C. C. Tsai, *Phys. Rev. B* **32**, 23 (1985).

10. T. J. McMahon and J. P. Xi, *Phys. Rev.B* **34**, 2475 (1986).

11. D. Redfield and R. H. Bube, *Phys. Rev. Lett.* **65**, 464 (1990).

12. R. Biswas, I. Kwon, and C. M. Soukoulis, *Phys. Rev. B* **44**, 3403 (1991).

13. M. Stutzmann, *Phil. Mag. B* **56**, 63 (1987).

14. M. Stutzmann, *Phil. Mag. B* **60**, 531 (1989).

15. J. Kakalios, R. A. Street, and W. B. Jackson, *Phys. Rev. Lett.* **59**, 1037 (1987).

16. W. B. Jackson, *Phys. Rev. B* **41**, 10257 (1990).

17. D. Adler, *Solar Cells* **9**, 133 (1982).

18. R. H. Bube, L. Benatar, and D. Redfield, *J. Appl. Phys.* **75**, 1571 (1994).

19. H. Fritzsche, *J. Non-Cryst. Solids* **6**, 49 (1971).

20. H. Overhof and W. Beyer, *Phil. Mag. B* **43**, 433 (1981).

21. H. M. Branz and M. Silver, *Phys. Rev. B* **42**, 7420 (1990).

22. B. von Roedern and A. Madan, *Phil. Mag. B* **63**, 293 (1991).

23. H. Overhof, *Mat. Res. Soc. Symp. Proc.* **258**, 681 (1992).

24. P. G. LeComber, A. Madan, and W. E. Spear, *J. Non-Cryst. Solids* **11**, 219 (1972).

25. R. H. Klazes, M. H. L. M. Van Den Broek, J. Bezemer, and S. Radelaar, *Phil. Mag.* **45**, 377 (1982).

26. M. H. Brodsky, M. A. Frisch, J. F. Ziegler, and W. A. Lanford, *Appl. Phys. Lett.* **30**, 561 (1977).

27. R. W. Collins, in *Amorphous Silicon and Related Materials*, edited by H. Fritzsche (World Scientific, Singapore, 1988), P. 1003.

28. C. R. Wronski, R. M. Dawson, M. Gunes, Y. M. Li, and R. W. Collins, *Mat. Res. Soc. Symp. Proc.* **297**, 443 (1993).

29. R. M. A. Dawson, C. M. Fortmann, M. Gunes, Y. M. Li, S. S. Nag, R. W. Collins, and C. R. Wronski, *Appl. Phys. Lett.* **63**, 955 (1993).

30. P V. Santos, W. B. Jackson and R. A. Street, *Phys. Rev. B* **44**, 12800 (1991).

31. M. Silver and R. C. Jarnagin, *Mol. Cryst.* **3**, 461 (1968).

32. H. Fritzsche, *J. Non-Cryst. Solids* **6**, 49 (1971).

33. H. Overhof and W. Beyer, *Phil. Mag. B* **43**, 433 (1981).

34. D. Han and H. Fritzsche, J. Non-Cryst. Solids **59-60**, 398 (1983).

35. H. M. Branz and M. Silver, *Phys. Rev. B* **42**, 7420 (1990).

36. B. von Roedern and A. Madan, *Phil. Mag. B* **63**, 293 (1991).

37. H. Overhof and P. Thomas, "Electronic Transport in Hydrogenated Amorphous Semiconductors" (Berlin, Springer-Verlag), **114**, 108 (1989).

38. S. D. Baranovskii and M. Silver, *Phil. Mag. Lett.* **61**, 77 (1990).

39. J. A. Howard and R. A. Street, *Phys. Rev. B* **44**, 7935 (1991).

40. C. Witt, U. Haken, M. Hundhausen, and L. Ley, *Verhandlungen DPG (VI)*, **30**, HL 26.2, Physik Verlag (1995).

41. B. von Roedern, *Am. Inst. Phys. Conf. Proc.* **234**, 122 (1991).

42. R. G. Palmer, D. l. Stein, E. Abrahams, and P. W. Anderson, *Phys. Rev. Lett.* **53**, 958 (1984)

43. E. H. Rhoderich and R. H. Williams, Metal- Semiconductor Contacts, (1988)

44. Wolfgang W. Gartner,*Phys. Rev.* **116**, 84 (1959).

REPORT DOCUMENTATION PAGE

Form Approved
OMB NO. 0704-0188

1. AGENCY USE ONLY (Leave blank)	2. REPORT DATE	3. REPORT TYPE AND DATES COVERED
	October 1996	Annual Subcontract Report, 15 May 1995 - 15 May 1996

4. TITLE AND SUBTITLE

Photocharge Transport and Recombination Measurements in Amorphous Silicon Films and Solar Cells by Photoconductive Frequency Mixing; Annual Subcontract Report, 15 May 1995 - 15 May 1996

5. FUNDING NUMBERS

C: XAN-4-13318-10
TA: PV631101

6. AUTHOR(S)

R. Braunstein and S. Dong

7. PERFORMING ORGANIZATION NAME(S) AND ADDRESS(ES)

University of California
Los Angeles, California

8. PERFORMING ORGANIZATION REPORT NUMBER

9. SPONSORING/MONITORING AGENCY NAME(S) AND ADDRESS(ES)

National Renewable Energy Laboratory
1617 Cole Blvd.
Golden, CO 80401-3393

10. SPONSORING/MONITORING AGENCY REPORT NUMBER

TP-451-21704

DE96013112

11. SUPPLEMENTARY NOTES

NREL Technical Monitor: B. von Roedern

12a. DISTRIBUTION/AVAILABILITY STATEMENT

12b. DISTRIBUTION CODE

UC-1262

13. ABSTRACT *(Maximum 200 words)*

Using the photomixing technique, we systematically studied the transport properties of intrinsic hydrogenated amorphous silicon (a-Si:H) samples that had hydrogen content ranging from over 10% to less than 1% and which were produced by the hot-wire technique at NREL. We investigated the continuous decay of electron drift mobility in intrinsic a-Si:H on light-soaking and determined the degradation of photoconductivity, lifetime, and drift mobility in these a-Si:H samples while light-soaking. In addition to the decay of the photoconductivity and electron lifetime, continuous decay of the electron drift mobility was found during the light-soaking process, which reveals a new phenomenon associated with the Staebler-Wronski effect. The drift mobility decreased by a factor of 2-4 for 5-hour light-soaking at 4-sun intensity. We investigated the effects of deposition conditions on transport properties of intrinsic a-Si:H films and, by using the photomixing technique, we determined the electron drift mobility, lifetime, and the conduction-band Urbach energy of a-Si:H films as a function of substrate temperature.

14. SUBJECT TERMS

photovoltaics ; amorphous silicon films ; photoconductive frequency mixing ; photocharge transport ; recombination measurements ; electron drift mobility ; Staebler-Wronski effect

15. NUMBER OF PAGES
49

16. PRICE CODE

17. SECURITY CLASSIFICATION OF REPORT	18. SECURITY CLASSIFICATION OF THIS PAGE	19. SECURITY CLASSIFICATION OF ABSTRACT	20. LIMITATION OF ABSTRACT
Unclassified	Unclassified	Unclassified	UL